1-1-2017

Uv-Induced Somatic Mutations Elicit A Functional T Cell Response In The Yummer1.7 Mouse Melanoma Model

Jake Xiao Wang
Yale University

UV-induced Somatic Mutations Elicit a Functional T Cell Response in the YUMMER1.7 Mouse Melanoma Model

A Thesis Submitted to the
Yale University School of Medicine
in Partial Fulfillment of the Requirements for the
Degree of Doctor of Medicine

by

Jake Xiao Wang

2017

Abstract

Human melanomas exhibit relatively high somatic mutation burden compared to other malignancies. These somatic mutations may produce neoantigens that are recognized by the immune system, leading to an anti-tumor response. By irradiating a parental mouse melanoma cell line carrying three driver mutations with UVB and expanding a single cell-derived clone, we generated a mutagenized model that exhibits high somatic mutation burden. When inoculated at low cell numbers in immunocompetent C57BL/6J mice, YUMMER1.7 (YUMM Exposed to Radiation) regresses after a brief period of growth. This regression phenotype is dependent on T cells as YUMMER1.7 tumors grow significantly faster in immunodeficient *Rag1*$^{-/-}$ mice and C57BL/6J mice depleted of CD4 and CD8 T cells. Interestingly, regression can be overcome by injecting higher cell numbers of YUMMER1.7, which results in tumors that grow without effective rejection. Mice that have previously rejected YUMMER1.7 tumors develop immunity against higher doses of YUMMER1.7 tumor challenge. Additionally, escaping YUMMER1.7 tumors are sensitive to anti-CTLA-4 and anti-PD-1 therapy, establishing a new model for the evaluation of anti-tumor immune responses and novel therapeutics.

Acknowledgements

I would like to thank Dr. Marcus Bosenberg and Dr. Richard Edelson for their incredible mentorship, support and enthusiasm for science. I am forever grateful to them for helping me discover my own passion.

I am indebted to every member of the Bosenberg and Edelson labs. In particular, I am deeply appreciative of Katrina Meeth, Alessandra Ventura and Curtis Perry, who are incredible teachers, colleagues and even better friends.

This work was supported by the Yale Office of Student Research and funded by the Howard Hughes Medical Institute Medical Research Fellows Program.

Table of Contents

Introduction

Mutational Landscape of Melanoma

During the year of Napoleon's Prussian Campaign in 1806, René Laennec provided the first description of melanoma as a disease in an unpublished memoir to the Faculté de Médecine in Paris (1). The first to use the word "melanoma," Laennec noted that this disease caused metastases in the mediastinal and hilar lymph nodes, which differed from bronchial glands blackened by carbon deposition. In 1820, William Norris made several observations about the possible genetic basis of melanoma: "it is remarkable that this gentleman's father…died of a similar disease. This tumor…originated in a mole and it is also worth mentioning that, not only my patient and his children had many moles…but also his own father and brothers…These facts…would incline me to believe that this disease is hereditary" (2). Since then, the neural crest-derived melanocyte has been identified as the cell of origin of melanoma, and breakthroughs have led to a fundamental understanding of the molecular drivers of melanoma.

Indeed, a proportion of melanomas are hereditary as evidenced by patients with familial atypical mole/melanoma syndrome (FAMM). In 1992, mutations in the *CDKN2A* gene were reported in a subset of kindreds with FAMM (3). This high-penetrance susceptibility gene locus encodes for two proteins, p16 and $p14^{ARF}$, which regulate cell cycle progression through the retinoblastoma and p53 pathways, respectively. In families, carriers of the *CDKN2A* mutation have an estimated risk of 30% to develop melanoma by age 50 and 67% by age 80 (4). In contrast to this high-risk allele, loss-of-function mutations in melanocortin 1 receptor (*MC1R*) modestly increase the susceptibility to melanoma in the

broader population with light complexion, red hair and blue eyes. UV irradiated keratinocytes secrete α-melanocyte stimulating hormone (αMSH), which binds to MC1R on melanocytes. MC1R activation of microphthalmia-associated transcription factor (MITF) induces melanocytes to produce brown/black eumelanin and red pheomelanin. Eumelanin protects against UV radiation, but pheomelanin can actually contribute to melanomagenesis through the production of reactive oxygen species (ROS) (5). Fair skin and red hair individuals with mutations in *MC1R* synthesize greater levels of pheomelanin compared to eumelanin and are at greater risk for melanoma development.

Other driver mutations known to induce carcinogenesis have been elucidated in melanoma. *BRAF* mutations occur in over 80% of melanocytic nevi and the valine-to-glutamic acid substitution at codon 600 is found in approximately 50% of melanomas (6). Although recent studies corroborate the role of ultraviolet radiation in all evolutionary stages of melanoma, $BRAF^{V600E}$ mutations are usually caused by T->A transversions, not typical of UV radiation (7, 8). $BRAF^{V600E}$ could be a direct but rare byproduct of UV radiation caused by error-prone DNA polymerases or the result of another mutagenic mechanism. Although a *BRAF* mutation alone typically is associated with benign melanocytic nevus formation and does not lead to malignant transformation, other genetic alterations cooperate with *BRAF* activation to induce melanomas. For instance, $Braf^{V600E}$ alone caused benign melanocytic hyperplasia, but rapidly resulted in melanoma when combined with *Pten* loss in a murine model (9). *PTEN* acts as a tumor suppressor by encoding a protein phosphatase that negatively regulates the PI3K/AKT pathway through its action on phosphatidylinositol phosphate (PIP_3). PI3K signaling promotes cell growth and survival. Loss of *PTEN* occurs in

20-30% of melanoma tumors. Similarly, *MITF* is also a melanoma oncogene that can transform melanocytes in conjunction with *BRAF*^{V600E} (10).

Additional driver mutations in melanoma include alterations in RAS proteins such as NRAS, KRAS and HRAS as well as c-KIT, which is the receptor tyrosine kinase for stem cell factor (SCF). These mutations are associated with different forms of clinical melanoma. For instance, *BRAF* and *NRAS* mutations are commonly found in superficial spreading and nodular melanoma while acral lentiginous melanomas generally harbor changes in *KIT*. Moreover, chronically sun-exposed melanomas are associated with *BRAF*^{nonV600E}, *NRAS* or *NF1* mutations whereas non-chronically sun-exposed melanomas affect younger individuals and are often driven by *BRAF*^{V600E} mutations (11). Contrastingly, uveal melanomas possess activating mutations in *GNAQ* and *GNA11*, which are also involved in MAPK signaling.

Compared to other cancer types, melanomas exhibit high rates of somatic mutations. Primary and metastatic melanomas are among the most highly mutated tumors analyzed by the Cancer Genome Atlas with a reported mean mutation rate of 16.8 mutations/Mb per exome (12). Primary melanomas generally carry more than one hundred nonsynonymous coding mutations per tumor (13). Accompanying driver mutations are a large number of passenger mutations that do not confer a selective growth advantage (14). The vast majority of these passenger mutations show a predominant UV signature (C -> T transitions at dipyrimidine sites) in melanoma.

Because passenger mutations dominate the melanoma genome landscape, they have the greatest potential to produce peptide epitopes that act as neoantigens and elicit anti-tumor immune responses (15). Distinct from the class of non-mutated “self-antigens” such as MAGE antigens and Melan-A/MART-1, neoantigen recognition by T cells is not affected by

central tolerance. However, the understanding of neoantigens has been limited by the fact that most are unique to each tumor. In a study of eight CD4 T cell neoantigens and thirteen CD8 T cell neoantigens, 20/21 epitopes were found in only one tumor from a cohort of approximately 20,000 human tumor samples (16). Nevertheless, high-throughput sequencing technologies now permit the identification of potential neoantigens on an individual basis. This is achieved by predicting major histocompatibility complex (MHC) binding peptides from nonsynonymous exonic mutations unique to the tumor and assessing for T cell reactivity. Predicted peptides can be filtered for expression and further prioritized based on likelihood of proteasomal processing, transport into the endoplasmic reticulum, affinity for MHC class I and II alleles and immunogenicity (based on the type of residues exposed to T cell receptors). While *in silico* methods of predicting neoepitopes have improved markedly, experimental validation is still required to confirm specific neoepitopes. Therapeutics to stimulate neoantigen-specific T cell responses using checkpoint blocking antibodies, oncolytic viruses or synthetic vaccines are of great interest.

Immunotherapy in Melanoma

As the most deadly form of skin cancer, melanoma caused 9,710 deaths in the United States in 2014 (17). Until recently, systemic therapy failed to significantly prolong survival in advanced stage melanoma patients. The FDA approved dacarbazine in 1975, but the alkylating chemotherapy resulted in only partial responses with median survival ranging from 5-11 months, similar to untreated control patients. Next, targeted therapies aimed at $BRAF^{V600E}$ patients improved response rates significantly. A randomized phase III trial showed that vemurafenib increased overall response rates to 48% compared to 5% for

dacarbazine (18). Subsequently, vemurafenib and dabrafenib, two BRAF inhibitors, were approved in 2011 and 2013, respectively. Unfortunately, despite high response rates, targeted therapies exhibit limited durability because of drug resistance. Mechanisms of resistance include reactivation of MAPK signaling through *MEK1*-activating mutations, *NRAS* mutations, loss of *NF1* or upregulation of PI3K signaling. BRAF inhibitors are now given in combination with MEK inhibitors to combat resistance and overcome paradoxical hyperactivation of CRAF in cells containing wild-type BRAF, which causes hyperproliferation of keratinocytes and low-grade squamous cell carcinomas. Nonetheless, the median progression-free survival for BRAF and MEK inhibitors remains only five to seven months (19).

In contrast, immunotherapy has demonstrated promising efficacy in advanced melanoma with a proportion of patients experiencing long-term survival. The first immunotherapy to be approved for metastatic melanoma was high dose interleukin-2 in 1998, which produced only an overall objective response rate of 16% and was associated with significant toxicities (20). Subsequently, checkpoint inhibitors, which block inhibitory pathways affecting T cell responses, achieved greater success. Activation of naïve T cells requires not only recognition of the MHC-peptide complex by the T cell receptor (TCR) but also costimulation, which amplifies TCR signaling. One costimulatory molecule on T cells is CD28, which binds B7 molecules (CD80 and CD86) on antigen-presenting cells. Contrastingly, cytotoxic T lymphocyte antigen-4 (CTLA-4) and programmed cell death-1 (PD-1) are inhibitory T cell receptors that suppress immune responses and play a role in tolerance. Tumors may be able to evade immunosurveillance by taking advantage of these two “brakes.”

CTLA-4 counteracts the early stages of T cell activation by binding B7 molecules with much higher affinity than CD28, thereby blocking costimulation (21, 22). CTLA-4 is also a target of the Forkhead Box P3 transcription factor (FOXP3), which determines the cell lineage of regulatory T cells. Thus, CTLA-4 may also enhance the immunosuppressive effects of regulatory T cells (23). These studies led to the development of ipilimumab, a monoclonal antibody (IgG1) against CTLA-4. In a landmark phase III clinical trial, metastatic melanoma patients treated with ipilimumab exhibited a median overall survival of 10.1 months compared with 6.4 months among patients receiving the cancer vaccine glycoprotein 100 (24). More importantly, in the 15 patients who had a partial or complete response, 9 maintained the response for at least 2 years. Grade 3 or 4 immune-related adverse events usually affecting the skin or gastrointestinal tract did occur in 10-15% of patients on ipilimumab including 7 associated deaths. But the durability of response to ipilimumab from this trial led to its approval in 2011. Since then, long-term responses to this therapy have been observed in approximately 20% of treated patients.

While both interfere with T cell responses, the mechanisms of PD-1 and CTLA-4 action differ significantly. Whereas anti-CTLA-4 promotes broad T cell activation that may not be specific for tumor antigens, anti-PD-1 targets effector T cell activity in peripheral, inflamed tissues because PD-1 ligands have limited distribution in normal tissues. Its major ligand, PD-L1, is expressed on tumor cells and other cells of the tumor microenvironment after exposure to T cells that secrete the cytokine interferon-γ (IFN- γ). For this reason, it is believed that PD-L1 is upregulated in response to cancer-induced inflammation, serving as negative feedback to quell immune responses. Such a regulatory system limits tissue damage during inflammation but also hinders tumor immunity (25). Altogether, data suggest that

anti-PD-1 therapy would induce less autoimmune toxicity than anti-CTLA-4. For this reason, clinical testing with PD-1 inhibitors was pursued.

Two human antibodies targeting PD-1, pembrolizumab and nivolumab, have demonstrated improved response rates in melanoma with less toxicity than ipilimumab. In a trial comparing nivolumab and dacarbazine, 40.0% of advanced melanoma patients treated with nivolumab achieved an objective response, significantly higher than the 13.9% response rate of patients on dacarbazine (26). The overall survival at 1 year was 72.9% in the nivolumab group and 42.1% in the dacarbazine group. Treatment-related adverse events of grade 3 or 4 occurred in 11.7% of patients on nivolumab. Likewise, in a head-to-head comparison within the KEYNOTE-006 trial, pembrolizumab increased response rates to 32.9-33.7% (two and three week regimens) from 11.9% with ipilimumab and prolonged overall survival (27). One year survival rates were 68.4%-74.1% in the pembrolizumab group and 58.2% for the ipilimumab group. Although 80.5% of patients had tumors positive for PD-L1 (defined as at least 1% of tumor cells staining positive for membranous PD-L1), the benefit of pembrolizumab over ipiliumab was observed in both PD-L1 positive and negative subgroups. Grade 3 to 5 adverse events occurred in 10.1-13.3% and 19.9% of patients receiving pembrolizumab and ipilimumab, respectively. Both nivolumab and pembrolizumab were approved by the FDA in 2014 for metastatic melanoma after progression on ipilimumab or a BRAF inhibitor.

Since anti-CTLA-4 and anti-PD-1 therapies take advantage of different mechanisms of T cell suppression, there was impetus to use them in combination. Indeed, multiple trials report the synergistic benefit of this combination in boosting response but at the cost of greater toxicities (28, 29). Nivolumab and ipilimumab produced an objective response rate of

61% compared to 11% in the ipilimumab group in one study (30). However, drug-related adverse events of grade 3 or 4 increased from 24% to 54%. Such events were the most common reason (45%) for discontinuation of the combination therapy. Thus, the higher response rates of combination treatment must be weighed against its safety profile.

Although immunotherapy has been successful in treating a variety of tumor types, they are particularly efficacious in melanoma. A major reason for this may be the high somatic mutation burden characteristic of melanoma (31). This hypothesis is supported by the success of a phase 2 clinical trial using PD-1 blockade to treat mismatch repair-deficient colorectal and non-colorectal cancers, which have even higher mutation loads than melanoma (32). Indeed, greater somatic mutations appear to be associated with improved survival in the setting of immune checkpoint blockade (33, 34). McGranahan et al. analyzed 64 melanoma patients treated with CTLA-4 antibody. Tumors exhibiting high clonal neoantigen burden and low neoantigen intratumoral heterogeneity exhibited significantly improved overall survival (35). Additionally, in two patients who responded to anti-CTLA-4 therapy, peripheral blood mononuclear cell analysis identified CD8 T cell populations that recognized neoantigens present in 100% of cancer cells. They reasoned that neoantigen burden influences sensitivity to immunotherapies, but the presence of such neoantigens on most tumor cells (homogeneity) is also important in predicting response.

Mouse Models of Melanoma

Mouse models of melanoma have long been utilized to advance our understanding of the disease. The first models were generated spontaneously from inbred mouse strains or induced with mutagens such as UV radiation or 7,12-Dimethylbenz(a)anthracene (36). One

of the spontaneously arising mouse melanomas first isolated over 86 years ago—the B16 cell line—remains widely used today in experimental studies (37). The ease with which it can be cultured, manipulated *in vitro*, and transplanted into congenic mice makes it a tractable model to study melanoma biology. Nevertheless, genetic drivers of B16 may not accurately reflect those present in human melanoma. Exome sequencing of B16F10 murine melanoma cells revealed 962 nonsynonymous somatic point mutation differences compared to the background C57BL/6 exome (38). Although homozygous deletion of *Cdkn2a* and two missense mutations in *Pten* were detected, no mutations were found in *Braf*, *c-Kit*, *Nras* or *Kras*. Furthermore, the study of immune responses generated against B16 tumors is also limited by several factors. First, retroviral elements appear to be important for B16 tumor formation, thereby confounding the generalizability of the model (39, 40). Also, B16 is considered to be poorly immunogenic given its low expression of MHC class I molecules (41). In fact, when CTLA-4 blockade was studied in this model, treatments showed little effect (42). Only when combined with a granulocyte/macrophage colony-stimulating factor (GM-CSF) expressing tumor cell vaccine did treatments induce rejection of the B16 tumors. Because of these caveats to B16, improved mouse melanoma models are necessary.

To accurately model driver mutations, transgenic mouse technology allows for the manipulation of molecular pathways commonly defective in melanoma. Genetically engineered mice are able to develop tumors through melanocyte-specific activation of the Ras or c-Met-HGF/SF signaling axes in combination with changes to cell-cycle control elements like p16 or p19. Furthermore, Cre-lox recombination allows the generation of conditional alleles, providing greater control over tumor formation. Dankort et al. described a mouse melanoma model with a $Braf^{V600E}$ mutation and *Pten* inactivation, which developed

melanomas upon administration of topical 4-hydroxytamoxifen (9). Their construct contained wild-type exons 15-18 of human *BRAF* flanked by loxP sites followed by the mutated exon 15 after the stop codon. So, when CreER was activated by tamoxifen via a Cre recombinase-estrogen receptor fusion transgene under the control of a tyrosinase promoter, the human exons were removed and the V600E mutated fully murine *Braf* allele was expressed under the control of its endogenous regulatory elements. The $Pten^{lox/lox}$ alleles conditionally deleted either exons 4 and 5 or only exon 5, which are critical for the phosphatase activity of the protein product. Although $Braf^{V600E}$ alone caused only benign melanocytic hyperplasia, the combination of $Braf^{V600E}$ and *Pten* silencing induced melanomas with 100% penetrance, no measurable latency, remarkable multiplicity, and metastases to the lymph nodes and lungs. Like this *Braf/Pten* model, other genetically engineered mouse models (GEMMs) have been created with genetic changes relevant to human melanoma (43, 44). These resources serve as valuable tools to study genotype-phenotype correlation.

To enhance the practicality of GEMMs, the Bosenberg lab has recently generated cell lines from genetically distinct melanoma GEMMs (45). Each cell line contains different combinations of genetic drivers (Table 1). They eliminate the need to maintain complex mouse colonies with the appropriate genotypes and can be implanted into congenic C57BL/6 mice to form tumors with shorter latency than GEMMs. This series, entitled the Yale University Mouse Melanoma (YUMM) cell lines, includes 10 different human-relevant genotypes. For example, YUMM1.1 was the first cell line derived from a tumor in a GEMM with the conditional alleles $Braf^{V600E/wt}$, $Pten^{-/-}$, $Cdkn2a^{-/-}$. YUMM1.7 has the same genotype as YUMM1.1 but was generated from a separate mouse and tumor. When evaluated *in vitro* and *in vivo*, *Braf*-driven YUMM lines were growth inhibited by treatment with PLX4720, a

Braf inhibitor. PLX4720 chow delayed growth of YUMM1.7 tumors until about day 50, after which growth rapidly increased. This demonstrated that the YUMM lines could be used to model clinical responses of human melanoma to targeted therapy. The YUMM series has been utilized widely and is being distributed by the American Type Culture Collection (ATCC) (46-48).

The original YUMM lines are only partially immunogenic based on immune infiltration, which consisted of mostly F4/80 tumor-associated macrophages and few CD3 T cells (45). Moreover, when YUMM1.7 was engrafted into wild-type C57BL/6 and immunodeficient *Rag1*$^{-/-}$ C57BL/6 mice, no significant differences in tumor growth were observed. In other words, an intact adaptive immune system did not effectively control tumor volume. The minimal immune response generated against these cell lines is likely due to their low somatic mutation burden as is the case in GEMMs. The purpose of the following work is to build a more immunogenic model using a YUMM cell line in order to retain the driver mutations important in human melanoma. Toward this end, we hypothesized that UV-induced passenger mutations would create additional neoantigens within cell lines and stimulate a more robust immune response. We show that a derivative of YUMM1.7 transformed through UV mutagenesis, YUMMER1.7 (YUMM Exposed to Radiation), indeed elicits a functional adaptive immune response dependent on T cells. This model better recapitulates the genomic landscape of human melanomas and responds to existing immune checkpoint therapies, setting the stage for future evaluation of novel therapeutics.

Table 1. Yale University Mouse Melanoma (YUMM) Cell Lines.

Each cell line family is designated by the first number, which corresponds to a particular combination of mutations that drives tumor formation. The second number identifies the individual tumor from which each cell line was derived.

Cell Line Family	Genotype	Individual Cell Lines
YUMM1	*Braf*$^{V600E/wt}$, *Pten*$^{-/-}$, *Cdkn2a*$^{-/-}$	YUMM1.1, 1.2, 1.3, 1.4, 1.5, 1.6, 1.7, 1.8, 1.9, 1.10, 1.11, 1.12, 1.13, 1.14, 1.15
YUMM2	*Braf*$^{V600E/wt}$, *Pten*$^{-/-}$, *Cdkn2a*$^{-/-}$, *Bcat*$^{STA/wt}$	YUMM2.1, 2.2
YUMM3	*Braf*$^{V600E/wt}$, *Cdkn2a*$^{-/-}$	YUMM3.1, 3.2, 3.3, 3.4
YUMM4	*Pten*$^{-/-}$, *Cdkn2a*$^{-/-}$	YUMM4.1, 4.2, 4.3, 4.4
YUMM5	*Braf*$^{V600E/wt}$, *p53*$^{-/-}$	YUMM5.1, 5.2, 5.3, 5.4
YUMM6	*Braf*$^{V600E/wt}$, *Pten*$^{-/-}$	YUMM6.1
YUMM7	*Braf*$^{V600E/wt}$, *Cdkn2a*$^{-/-}$, *Bcat*$^{STA/wt}$	Future lines
YUMM8	*Braf*$^{V600E/wt}$, *Cdkn2a*$^{-/-}$, *Lkb1*$^{-/-}$	Future lines
YUMM9	*Nras*^{Q61R}, *Cdkn2a*$^{-/-}$,	Future lines
YUMM10	*Nras*^{Q61R}, *p53*$^{-/-}$	Future lines

Hypothesis:

Somatic mutations induced by UV irradiation of a mouse melanoma model elicit a robust T cell dependent anti-tumor response that can be modulated with immunotherapeutics.

Specific Aims:

Specific Aim 1: Derive a mouse melanoma model with high somatic mutation burden from a parental cell line by UV mutagenesis.

Specific Aim 2: Characterize the immune response against the mutagenized melanoma tumor model.

Specific Aim 3: Evaluate the responsiveness of the mutagenized melanoma model to immune checkpoint blockade.

Methods

All procedures, experiments and analyses were conducted by the author unless otherwise specified.

Cell lines and tissue culture

YUMMER1.7 was derived from YUMM1.7, which was generated from a GEMM containing the alleles *Braf*$^{V600E/wt}$, *Pten*$^{-/-}$, *Cdkn2a*$^{-/-}$ (45). Irradiation of YUMM1.7 included three rounds of 1500J/m^2 UVB (3W for 500 sec) when cells were 50-70% confluent. Cells were given time to recover and proliferate before being re-plated and proceeding to the next UV treatment. After the final UV treatment, a single cell was clonally expanded. UV irradiation and clonal expansion of the cell line were done by Katrina Meeth. YUMM1.7 and YUMMER1.7 DNA content were assessed using a Propidium Iodide Flow Cytometry Kit according to manufacturer instructions (Abcam, Cambridge, UK). YUMMER1.7-GFP and YUMM1.7-GFP were generated using a P-YUK-GFP plasmid with PiggyBac Transposase Expression Vector, a gift from Tian Xu, Department of Genetics, Yale University. Transfection was done with Lipofectamine 2000 (Invitrogen, Carlsbad, California) and cells were selected using Blastomycin resistance. All cell lines were maintained in DMEM/F12 media containing 10% FBS, 1% nonessential amino acids and 1% penicillin-streptomycin.

***In vivo* mouse studies**

Four to six week old C57BL/6J mice were purchased from the Jackson Laboratory (Bar Harbor, ME) and allowed to acclimate for one week prior to use. C57BL/6J *Rag1*$^{-/-}$ mice were also obtained from the Jackson Laboratory and maintained in our mouse colony. All animal experiments protocols were followed according to the Yale Office of Animal Research Support Committee guidelines. For tumor inoculation, YUMM1.7 and YUMMER1.7 cells were harvested at approximately 60-85% confluence on the day of injection. Cells were trypsinized with 0.25% trypsin for approximately 2-3 minutes before deactivation with media containing 10% serum. They were then washed twice with sterile 1x PBS and counted with an Invitrogen Countess or with a hemocytometer. Cells in 100 µL of sterile PBS were injected subcutaneously into a shaved rear flank using a 27G needle. Mice were monitored for the appearance of tumor after injection to begin digital caliper measurements. Three dimensions were taken for calculation of tumor volume, which was calculated using the equation: 0.5233*l*w*h. For depletion experiments, antibodies for CD4 (GK1.5) and CD8 (TIB210) were made in-house using hydridomas. Mice were injected with 10 mg/kg of each antibody on day -1 and then twice per week for the course of treatment. Loss of CD4 and CD8 T cells were verified by flow cytometry. For immunotherapy treatments, anti-CTLA-4 (9H10), anti-PD-1 (RMP1-14), anti-PD-L1 (10F.9G2) antibodies were purchased from Bio X Cell (West Lebanon, NH) along with the corresponding isotype controls, Syrian Hamster IgG2, Rat IgG2a and Rat IgG2b respectively. Treatments were started with palpable tumors at 6 days after initial cell line injections. Mice were given 10 mg/kg anti-CTLA-4, anti-PD-1 or anti-PD-L1 three times per week for four weeks. CSF-1R inhibitor chow (PLX6134, Plexxikon, Berkeley, CA and ResearchDiets, New Brunswick,

NJ) was administered at a concentration of 800 mg/kg for the duration of the treatment course. Treatments and tumor measurements for the PD-L1 and CSF-1R inhibitor experiment were completed by William Damsky.

Histological analysis

At least three tumors were fixed in 10% formalin for each condition—100,000 cell YUMM1.7-GFP, 100,000 cell YUMMER1.7-GFP and 500,000 cell YUMMER1.7-GFP tumors at every time point—and embedded in paraffin. Cut sections were stained using GFP (Abcam 10558, Cambridge, UK), CD45 (Abcam 290, Cambridge, UK), F4/80 (Thermo Fisher 16363, Waltham, MA), CD3 (Biocare Medical 215, Concord, CA), Foxp3 (eBioscience 145773, San Diego, CA), Cleaved Caspase-3 (Abcam 4051, Cambridge, UK) antibodies. Images of representative fields were taken of the tumor types and quantified at 40X magnification. The positive cells (brown) were counted and compared to the total nucleated cells in the field. Five fields were taken per tumor section and averaged.

Flow cytometry analysis

Single-cell suspensions from tumors or splenocytes were incubated with anti-Fc receptor antibody (2.4G2) on ice for 15 minutes in FACS buffer (PBS with 1% FBS and sodium azide). The cells were then stained with the appropriate antibodies in 2.4G2-containing FACS buffer on ice for 30 minutes. For intracellular cytokine staining, cells were fixed in Fix/Perm (eBioscience, San Diego, CA) and stained with antibodies to detect intracellular cytokines or transcription factors. All samples were evaluated with LSRII flow cytometers

and analyzed with Flowjo (Flowjo, LLC., Ashland, Or). Antibodies against CD45 (A20), CD8 (53-6.7) and CD3 (145-2C11) were purchased from eBioscience. Antibodies against CD4 (RM4-5), PD-1 (RMP1-14), and TIGIT (1G9) were purchased from Biolegend.

DNA Extraction and Exome Sequencing

DNA was extracted from YUMM1.7 and YUMMER1.7 cell lines as well as wild-type C57BL/6J mouse ears using Qiagen's DNeasy Blood & Tissue kit (Hilden, Germany). All samples passed quality control and were exome sequenced with 100 bp paired end reads using Agilent's SureSelectXT Mouse All Exon kit by Macrogen (Cambridge, MA). Analysis of the exome sequencing was conducted by Durga Thakral. Reads were aligned to the mm10 reference (ftp://ftp-mouse.sanger.ac.uk/ref/GRCm38_68.fa) using BWA version 0.7.15 with the –M option. Duplicate reads were marked with Picard version 2.6.0 MarkDuplicates. The resulting alignments were subjected to base quality score recalibration in GATK 3.6 using the *Mus musculari*s C57BL/6J SNP and Indel databases according to GATK best practices. Variants unique to YUMMER1.7 compared to YUMM1.7 or cell lines compared to wild-type C57BL/6J were called using GATK MuTect2 with the above mentioned dbsnp and mm10 references and were selected for downstream analysis if they passed the default MuTect2 filters. Then, variants were annotated using Annovar (2016Feb01 release) with the corresponding mm10 ensGene reference according to the program manual.

Statistical Analyses

Unpaired two-tailed t tests and Kaplan-Meier statistical analyses were performed using GraphPad Prism (Version 6.0a for Mac OS X, GraphPad Software, La Jolla, CA) using a significance cutoff; **ns** $p > 0.05$, $^{*}\ p \leq 0.05$, $^{**}\ p \leq 0.01$, $^{***}\ p \leq 0.005$.

Results

Specific Aim 1: Derive a mouse melanoma model with high somatic mutation burden from a parental cell line by UV mutagenesis.

As a part of the original YUMM series, the YUMM1.7 cell line carries three driver mutations: *Braf*$^{V600E/wt}$, *Pten*$^{-/-}$ and *Cdkn2a*$^{-/-}$. To generate the mutagenized mouse model, YUMMER1.7, YUMM1.7 was exposed to three rounds of UVB radiation (1500 J/m^2). After the last round of radiation, a single cell-derived clone was selected and expanded (Figure 1A).

In order to characterize the number of UV-induced somatic mutations in YUMMER1.7, whole exome sequencing of both the parental YUMM1.7 and mutagenized YUMMER1.7 cell lines were performed and compared to the wild-type C57BL/6J exome. YUMM1.7 exhibited 310 nonsynonymous exonic point mutations upon comparison to C57BL/6J (Table 2), which likely reflects incomplete backcrossing of the four alleles in the original genetically engineered mouse model. There were an additional 1446 unique nonsynonymous exonic mutations in YUMMER1.7 relative to YUMM1.7. A large proportion of these single-base changes (81.5%) were C>T transitions, which is consistent with ultraviolet light treatment and mutagenesis (Figure 1B). Upon evaluation of DNA content in the cell lines, it was determined that YUMM1.7 contains both diploid and tetraploid clones whereas YUMMER1.7 is tetraploid with twice the DNA content as splenocytes (Figure 2). Tetraploidy has been reported in melanoma. In one study, 65-90% of cells from 8/8 melanoma surgical specimens exhibited tetraploidy as evaluated by in situ hybridization (49).

Figure 1. Generation and Characterization of YUMMER1.7 Mutations.

(A) YUMMER1.7 was generated from YUMM1.7 using three rounds of UVB radiation, and a single cell-derived clone was expanded.

(B) Total point mutations in YUMMER1.7 compared to YUMM1.7 categorized based on the type of base substitution.

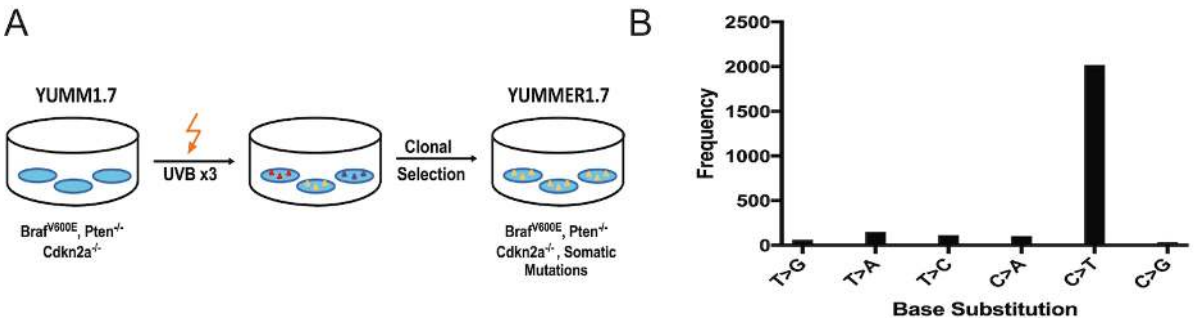

Figure 2. YUMMER1.7 is tetraploid.

Propidium iodide flow cytometry demonstrates that the vast majority of YUMM1.7 cells (orange) are diploid with similar DNA content as splenocytes (red) whereas YUMMER1.7 (blue) exhibits double the DNA content.

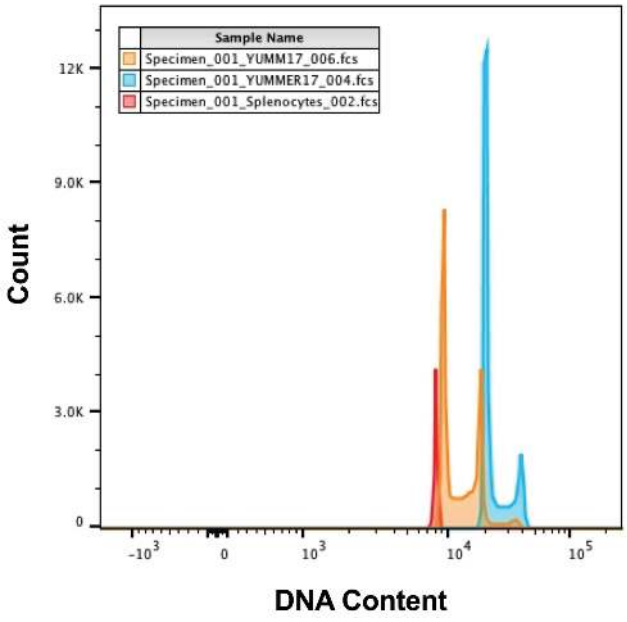

Table 2. Mutations between YUMM1.7 and YUMMER1.7 categorized by mutation type based on whole exome sequencing.

	Synonymous Mutations	Nonsynonymous Mutations	Other Mutations[A]	Mutational Load (total # of exonic mutations)
YUMM1.7 vs C57BL/6J	554	310	17	881
YUMMER1.7 vs C57BL/6J	1457	1731	120	3308
YUMMER1.7 vs YUMM1.7	924	1446	111	2481

[A]Frameshift indels, nonframeshift indels, stoploss, stopgain

Specific Aim 2: Characterize the immune response against the mutagenized melanoma tumor model.

In order to understand *in vivo* growth characteristics of YUMMER1.7 relative to YUMM1.7, we subcutaneously implanted 100,000 cells of each model into the flanks of C57BL/6J mice and measured tumor volume over time. As expected, YUMM1.7 tumors exhibited rapid and continuous growth (Figure 3A). In contrast, YUMMER1.7 cells initially grew to a palpable tumor of approximately 10-50 mm^3 followed by striking tumor regression without regrowth. Clinical regression of YUMMER1.7 melanomas (tumor volume decrease) was observed as early as 14 days post-injection, and complete regression was durable for at least 120 days.

Next, we implanted greater numbers of YUMMER1.7 cells in a similar fashion. Unlike the 100,000 cell injections, the inoculations of more than 250,000 YUMMER1.7 cells resulted in tumors that did not regress and eventually required euthanasia of the mouse, suggesting that tumor regression could be overcome by increasing the number of cells injected (Figure 3B). To further investigate why inoculation sizes of 100,000 YUMMER1.7 cells or less leads to tumor regression, we hypothesized that the phenomenon was immune mediated. Thus, we injected 100,000 YUMMER1.7 cells into the flanks of immunodeficient *Rag1*$^{-/-}$ mice that lack functional T and B cells. Interestingly, all YUMMER1.7 tumors (5/5) in *Rag1*$^{-/-}$ mice grew without any cases of regression (Figure 3C). Indeed, the YUMMER1.7 tumors grew at a similar rate compared to the parental model YUMM1.7 tumors. Antibody-mediated depletion of CD4 and CD8 T cells in wild-type C57BL/6J mice also increased tumor growth of YUMMER1.7 when 100,000 cells were injected (Figure 3D). We found that

depletion of both CD4 and CD8 T cells significantly accelerated tumor growth compared to the isotype control ($p = 0.006$). These results suggested that tumor regression was the result of an adaptive immune response involving both CD4 and CD8 T cells.

Subsequently, we explored whether mice that had rejected 100,000 cell YUMMER1.7 tumors would develop immunity against higher doses of YUMMER1.7 tumors (Figure 4). We injected 100,000 YUMMER1.7 cells into the right flanks of C57BL/6J mice and allowed tumors to completely regress after 30 days. This cohort was then rechallenged with 500,000 cell YUMMER1.7 (I + YUMMER1.7) or 500,000 cell YUMM1.7 (I + YUMM1.7) tumors on the left flanks. All five immunized mice rejected YUMMER1.7 tumors, whereas none rejected YUMM1.7 tumors. 4/5 tumors grew out in the control naïve C57BL/6J mice that were given the same 500,000 cell dose of YUMMER1.7. Interestingly, although all YUMM1.7 tumors grew out, the tumors were smaller in the I + YUMM1.7 group than in the N + YUMM1.7 group, albeit without reaching significance ($p = 0.19$). Finally, antibody-mediated depletion of CD4 and CD8 eliminated the effect of immunization as evidenced by 4/4 tumors failing to regress in the I + YUMMER1.7 + anti-CD4/CD8 group. These observations suggest that mice vaccinated with a low dose of YUMMER1.7 mounted an adequate T cell memory response to reject a higher burden of YUMMER1.7 tumors that would otherwise escape immune surveillance in naïve animals. The differences in YUMM1.7 tumor sizes in naïve and YUMMER1.7 immunized mice may be attributed to an immune response against the shared antigens between the two cell lines.

In addition, we sought to compare the intratumoral immune infiltration, mitotic rate and apoptotic cell death between YUMM1.7 and YUMMER1.7 tumors as a function of time. In order to track very early tumors, YUMM1.7 and YUMMER1.7 cell lines were labeled

with GFP, implanted and harvested at different time points—day 5, 10, 15, 20, 25 post-implantation for analysis by immunohistochemistry. Similar to the unlabeled lines, 100,000 cell YUMM1.7-GFP and 500,000 cell YUMMER1.7-GFP (YUMMER1.7-GFP^{HI}) tumors grew out whereas 100,000 cell YUMMER1.7-GFP (YUMMER1.7-GFP^{LO}) tumors regressed over time as shown by GFP staining as a percent of nucleated cells (Figure 5A). As a result of regression before day 25, staining for YUMMER1.7-GFP^{LO} tumors at day 25 is not available. The infiltration of CD45 and CD3 positive nucleated cells increased over time in YUMMER1.7-GFP^{LO} tumors whereas the percentage of these cells remained relatively constant or decreased in YUMMER1.7-GFP^{HI} and YUMM1.7-GFP tumors (Figure 5A, B). At day 20, a period when YUMMER1.7-GFP^{LO} is regressing and YUMMER1.7-GFP^{HI} and YUMM1.7-GFP are rapidly expanding, the fraction of CD45 positive nucleated cells were significantly greater in YUMMER1.7-GFP^{LO} than YUMMER1.7-GFP^{HI} ($p = 0.0045$) and YUMM1.7-GFP ($p = 0.0016$) tumors. Similarly, CD3 staining was increased in YUMMER1.7-GFP^{LO} tumors compared to YUMMER1.7-GFP^{HI} ($p = 0.0141$) and YUMM1.7-GFP ($p = 0.0574$) tumors. In YUMMER1.7-GFP^{LO} tumors, although CD3 infiltration increased over time, the amount of Foxp3 positive staining (a marker of immunosuppressive regulatory T cells) remained relatively low. This contrasts with increased Foxp3:CD3 ratio over time within YUMMER1.7-GFP^{HI} and YUMM1.7-GFP tumors (Figure 5B). Representative images of each cell line and condition are shown for the day 20 time point (Figure 5C). Additionally, the mitotic rate was low for all three tumor types until day 20, when mitosis markedly increased in YUMMER1.7-GFP^{HI} and YUMM1.7-GFP tumors only (Figure 5D). In contrast, cleaved caspase-3 staining, a marker

of apoptosis, progressively increased only in YUMMER1.7-GFP^{LO} tumors over time and remained low in both types of escaping tumors.

To further characterize the T cell infiltrate, tumors were harvested from wild-type C57BL/6J mice injected with either 500,000 YUMMER1.7 or 500,000 YUMM1.7 cells. Tumors were evaluated upon reaching 500-1000 mm^3 in volume for flow cytometry analysis (between day 30-40). Both CD4 ($p = 0.017$) and CD8 T cells ($p = 0.020$) were present at significantly higher numbers per gram of tumor in YUMMER1.7 implants compared to YUMM1.7 implants (Figure 6). Moreover, tumor-associated YUMMER1.7 CD8 T cells expressed increased activation/exhaustion markers such as PD-1 and TIGIT ($p = 0.0002$).

Figure 3. *In vivo* growth characteristics of YUMM1.7 and YUMMER1.7 in immunocompetent and immunodeficient C57BL/6J mice.

(A) Growth of 100,000 cell YUMM1.7 and YUMMER1.7 tumors engrafted into wild-type C57BL/6J mice.

(B) Growth of 100,000, 250,000, 500,000, and 1,000,000 cell YUMMER1.7 tumors engrafted into wild-type C57BL/6J mice.

(C) Growth of 100,000 cell YUMM1.7 tumors and YUMMER1.7 tumors engrafted into *Rag1*$^{-/-}$ C57BL/6J mice.

(D) Growth of 100,000 cell YUMMER1.7 tumors engrafted into wild-type C57BL/6J mice that were treated with depleting antibodies against CD4, CD8 or both.

Tumor growth curves are representative of two independent experiments (mean ± SEM, N = 5 each).

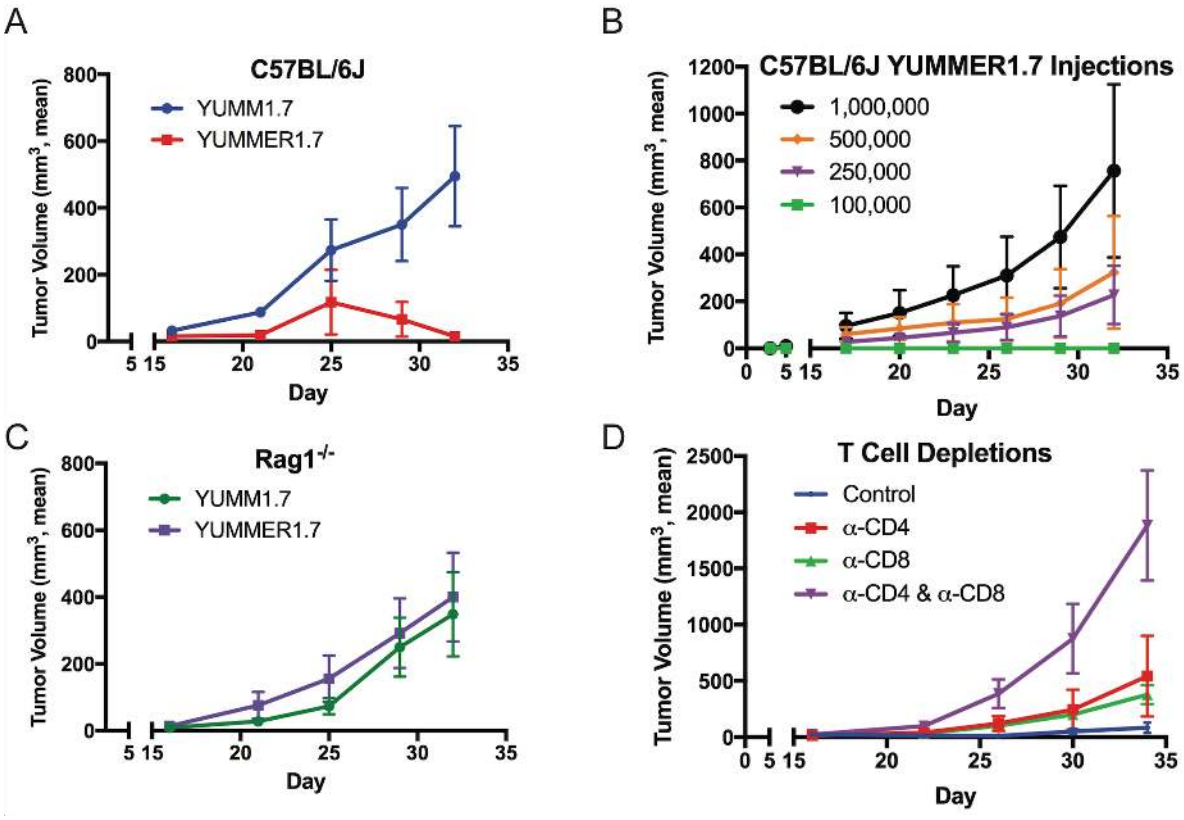

Figure 4. Rejection of tumors with low dose YUMMER1.7 immunizes against tumor rechallenge with high dose YUMMER1.7.

N = naïve C57BL/6J mice, I = C57BL/6J mice injected with 100,000 YUMMER1.7 cells and allowed to regress completely for 30 days prior to tumor rechallenge.

Tumor growth curves are representative of two independent experiments (mean ± SEM, N = 4-5 each).

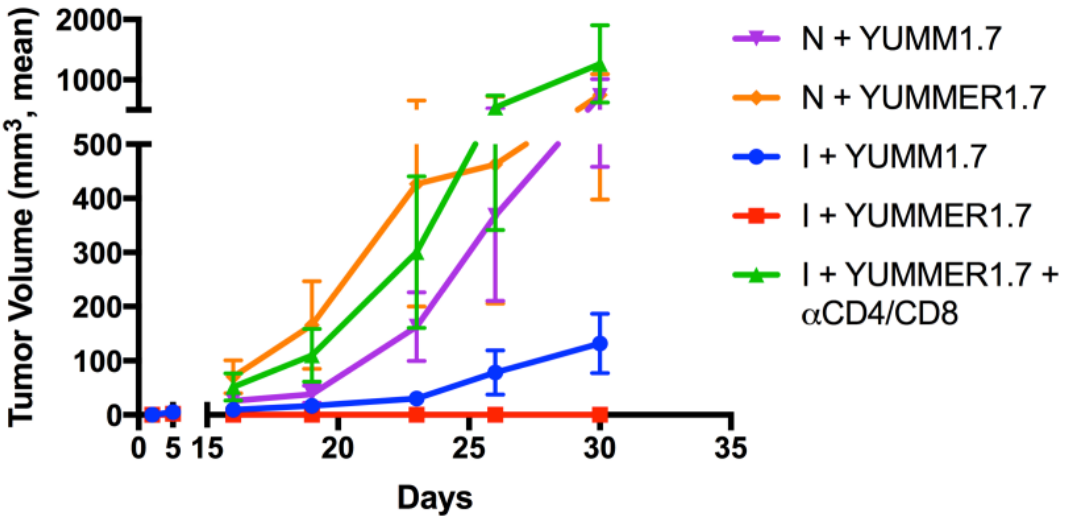

Figure 5. Immune infiltration, mitotic rate and apoptotic cell death within YUMM1.7-GFP and YUMMER1.7-GFP tumors.

(A) GFP (melanoma), CD45, CD3, F4/80-positive cells as a percent of nucleated cells.

(B) CD3, Foxp3 as a percent of nucleated cells and Foxp3 as a percentage of CD3 positive cells (orange).

(C) Representative immunohistochemical images of YUMM1.7-GFP and YUMMER1.7-GFP tumors on day 20 with the indicated staining at 40X magnification. YR^{LO} = YUMMER1.7-GFP^{LO}, YR^{HI} = YUMMER1.7-GFP^{HI}, YM = YUMM1.7-GFP.

(D) Mitotic rate and cleaved caspase-3 staining for YUMM1.7-GFP and YUMMER1.7-GFP tumors over time.

For Figure 5A, B, D, data are averages of counts from at least three independent tumors (mean ± SEM).

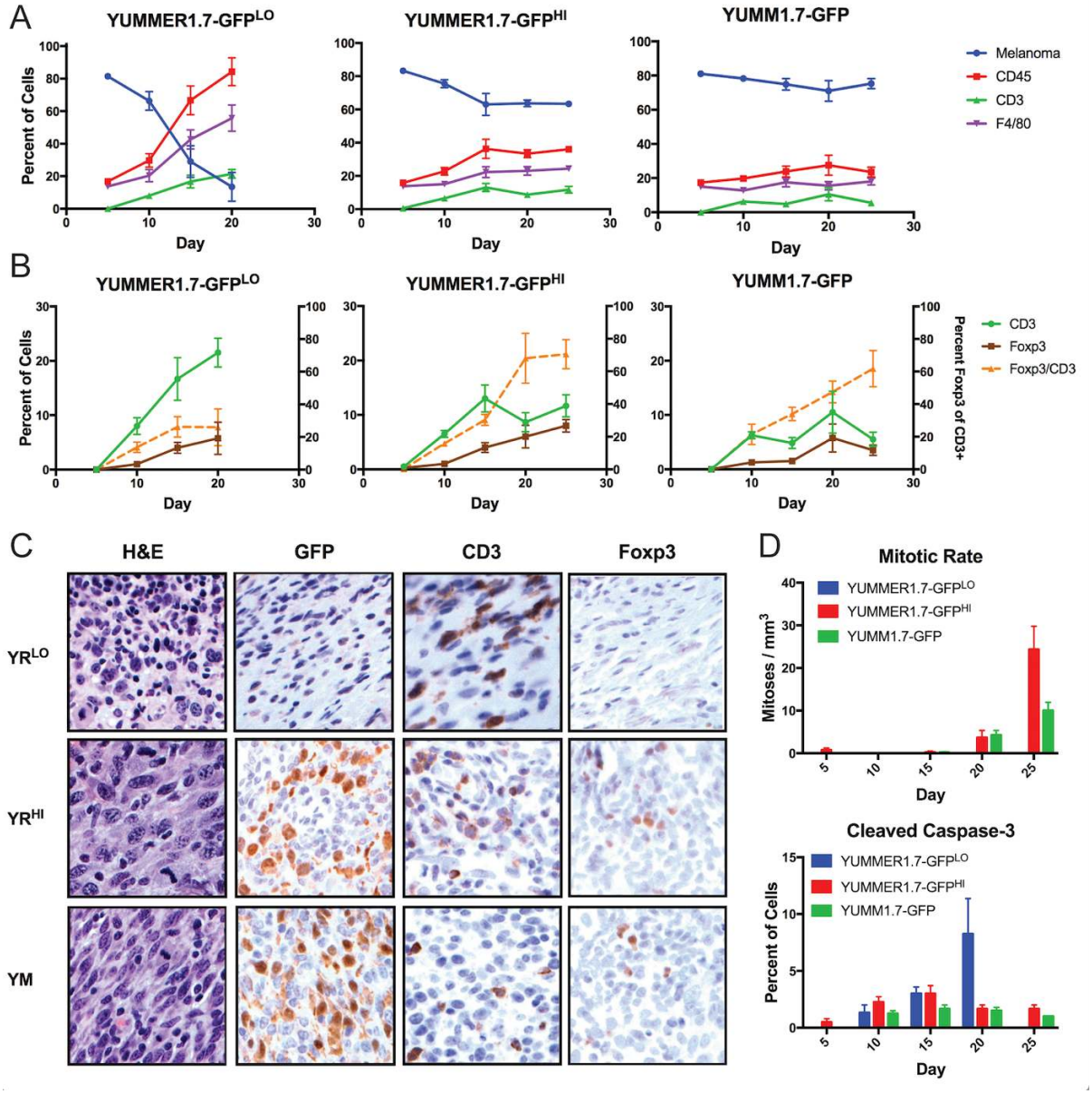

Figure 6. Immune infiltration of escaping YUMM1.7 and YUMMER1.7 tumors.

(A) Density of $CD4^+$ T cells per gram of tumor.

(B) Density of $CD8^+$ T cells per gram of tumor.

(C) Percent of $CD8^+$ T cells that are $PD1^+$ $TIGIT^+$.

500,000 cell YUMM1.7 and YUMMER1.7 tumors were harvested on day 30-40 for analysis by flow cytometry. Data are from two independent experiments (N=2-3 each). Mean ± SEM are shown.

* $p \leq 0.05$, *** $p \leq 0.005$.

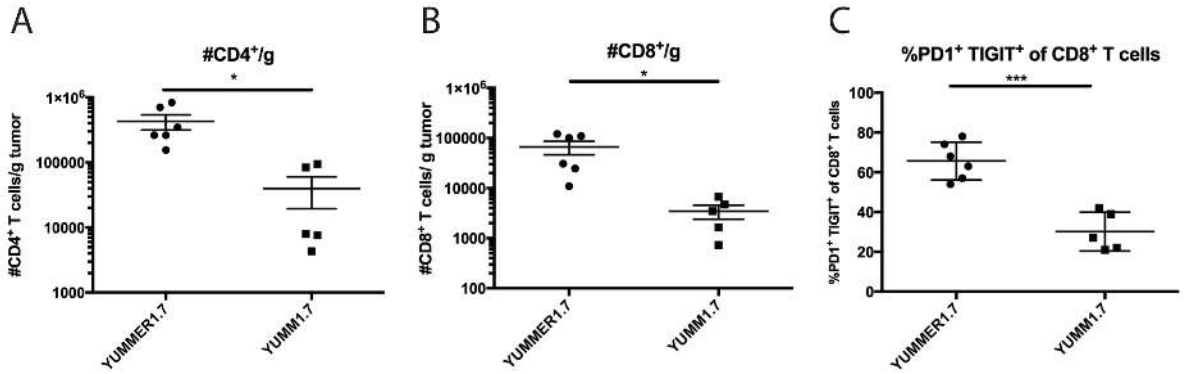

Specific Aim 3: Evaluate the responsiveness of the mutagenized melanoma model to immune checkpoint blockade.

Poor immunogenicity of existing syngeneic tumor models has hindered the study and evaluation of immunotherapies. We tested the effect of PD-1 and CTLA-4 blockade in the 500,000 cell YUMMER1.7 model, which would otherwise result in lethal tumor formation. All 5 mice in the isotype treated control group progressed to endpoint (tumor volume >1,000 mm^3) by day 32, whereas 4/5 anti-CTLA-4 treated tumors, 2/5 anti-PD-1 treated tumors and 5/5 combination treated tumors regressed completely (Figure 7A). When regression was complete, no tumors regrew for at least 180 days even after treatment was stopped. The one tumor in the anti-CTLA-4 treatment group that grew out was slowed by the therapy such that it did not reach endpoint until day 78 (Figure 7B). Both anti-CTLA-4 ($p = 0.0034$) and anti-PD-1 ($p = 0.0119$) treatments significantly delayed the progression of YUMMER1.7 tumors from 500,000 cell inoculations compared to the isotype control. Similarly, the combination of the two checkpoint inhibitors inhibited tumor growth versus isotype control ($p = 0.0034$). When single and combination treatments were compared against each other, only the PD-1 versus combination treatment comparison was borderline significant ($p = 0.0494$) in these small experimental groups. These effects were not seen in 500,000 cell YUMM1.7 tumors as combination treated tumors did not significantly differ in size from isotype antibody control treated tumors (Figure 7C).

The success of immune checkpoint blockade in the YUMMER1.7 model motivated us to test additional immunotherapy combinations. To overcome non-responsiveness or resistance to PD-1/PD-L1 inhibitors observed in patients, one approach is to target immunosuppressive tumor-associated macrophages. Indeed, in both the YUMM and

YUMMER1.7 models, F4/80+ macrophages comprise a large percentage of CD45+ hematopoietic cells within the tumor microenvironment. Thus, we treated 500,000 cell YUMMER1.7 tumors with anti-PD-L1, CSF-1R inhibitor or the combination of both (Figure 8). Preliminary experiments indicate that CSF-1R inhibitor enhances the anti-tumor effect of anti-PD-L1. Whereas 2/4 anti-PD-L1 treated tumors were growth delayed (no regression), 2/3 combination treated tumors regressed completely. CSF-1R inhibitor alone did not significantly delay tumor growth compared to the control group. These results illustrate the utility of YUMMER1.7 to provide preclinical rationale for novel therapeutics.

Figure 7. YUMMER1.7 but not YUMM1.7, is sensitive to checkpoint inhibitors anti-CTLA-4 and anti-PD-1.

(A) Individual tumor growth curves for YUMMER1.7 tumors treated with anti-CTLA-4, anti-PD-1 or both compared to isotype control. Data are representative of two independent experiments (N = 4-5).

(B) Kaplan-Meier survival curves for YUMMER1.7 and (C) YUMM1.7 treated tumors with an endpoint of tumor size >1000 mm^3 (N = 4-5).

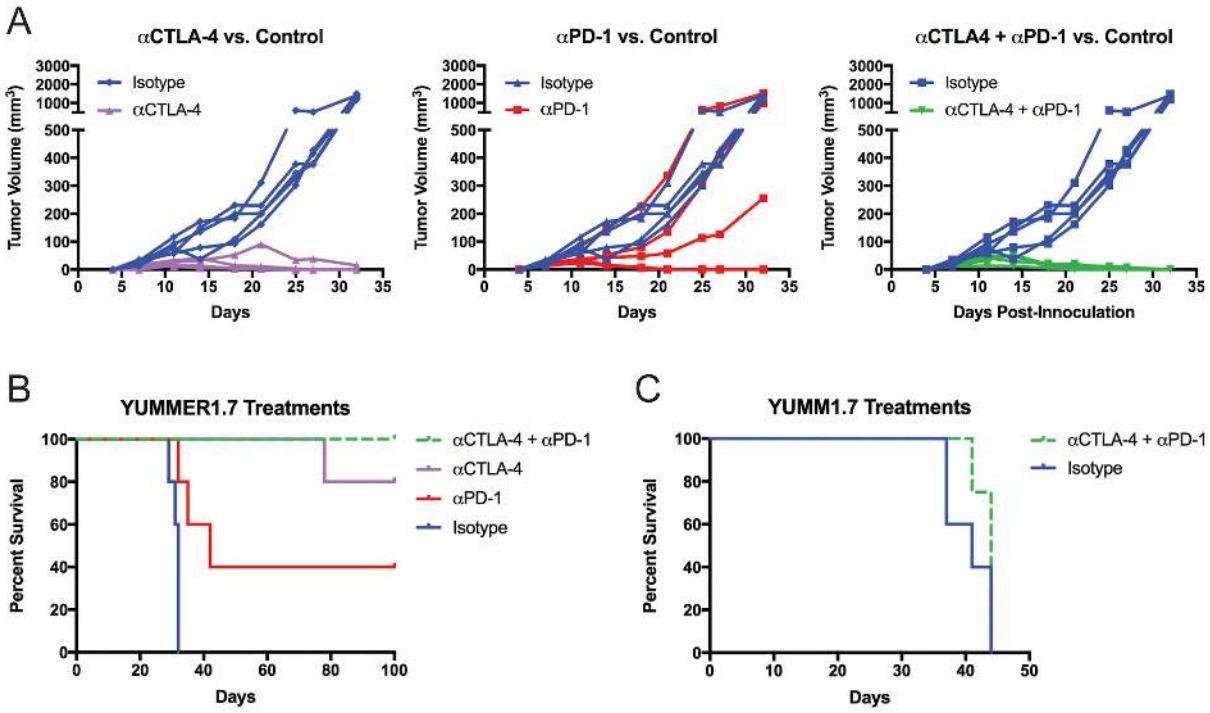

Figure 8. Combined inhibition of CSF-1R and PD-L1 is superior to either treatment alone in YUMMER1.7.

Individual tumor growth curves for YUMMER1.7 tumors treated with anti-PD-L1, CSF-1R inhibitor or both compared to control. Preliminary data from one experiment (N = 3-5).

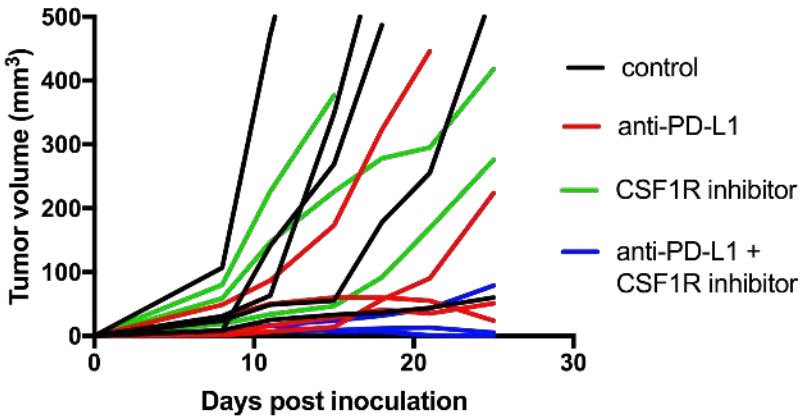

Discussion

Mouse models of cancer have been a tremendous resource for studying the biology of human malignancies (50). Although fundamental differences exist between species particularly with respect to immune function, progress in genetic engineering has helped improve models to more accurately reflect disease and the human host (51). Here, we describe the generation of a cell line designed to closely model the genomic features of human melanoma including common driver mutations and the high burden of passenger mutations. Since low somatic mutation burden in many mouse models can limit tumor immune responses and the study of immunotherapy, increasing antigen burden by UV irradiation was an important element in creating YUMMER1.7 (52). Unlike the parental YUMM1.7, which exhibits similar growth in the presence or absence of a functional adaptive immune system, YUMMER1.7 elicits a robust immune response as demonstrated by the quantity and quality of immune infiltration (45). More importantly, the difference in growth kinetics of YUMMER1.7 tumors in wild-type, *Rag1*$^{-/-}$ and T cell-depleted C57BL/6J mice suggests that the adaptive immune system may be responsible for YUMMER1.7 tumor regression when 100,000 or fewer cells are injected. What's more, this immune response confers protection against future rechallenge of high doses of YUMMER1.7 in vaccinated mice, likely a manifestation of T cell memory.

The phenotype of YUMMER1.7 tumor growth depends on the initial inoculation cell number. In contrast to inoculation cell numbers of 100,000 or less, when 250,000 or more cells are implanted, tumors grow out. Potentially, the increased inoculation cell number allows the mitotic rate of cancer cells to outpace or otherwise evade the developing immune response. Another possibility is that persistently high antigen levels in the context of sub-

optimal co-stimulation may lead to an anergic or exhausted T cell phenotype analogous to what has been reported in mice infected with chronic lymphocytic choriomeningitis virus (53). Furthermore, regulatory T cells may play a functional role as we observed that regressing tumors are characterized by lower Foxp3:CD3 ratios by IHC compared to tumors that grow out (Figure 2B). The Foxp3:CD3 ratio may be increased by indole 2,3-dioxygenase (IDO), which is known to promote conversion of naïve T cells to regulatory T cells and can be expressed by dendritic cells, myeloid derived suppressor cells and cancer cells (54). Reducing the regulatory T cell subset through an IDO inhibitor (1-methyl-D-tryptophan) or engraftment into $Foxp3^{DTR}$ mice may reduce the growth of YUMM1.7 and YUMMER1.7 tumors (55).

Despite the escape from regression, the 500,000 cell YUMMER1.7 tumors continue to be infiltrated by a significantly larger numbers of CD4 and CD8 T cells when compared to YUMM1.7 tumors. One possible explanation for this difference is that YUMMER1.7 neoantigens are more immunogenic than YUMM1.7 tumors. Indeed, the identification of neoantigens that elicit this immune response in this model is of great interest. Through exome sequencing and peptide prediction algorithms such as NetMHC, we have begun generating and ranking neoantigens based on affinity for the C57BL/6J MHC class I molecules, H-$2D^b$ and H-$2K^b$ (56). T cells reactive against neoantigens from 100,000 cell YUMMER1.7 vaccinated mice can then be tested using tetramer based assays with the predicted epitopes. For example, Gubin et al. utilized a similar method to identify two mutant antigens responsible for rejection of sarcoma tumors upon treatment with anti-PD-1 (57). They discovered that tumor-infiltrating CD8 T cells bound to fluorescently labeled tetramers loaded with these two peptides and that T cells from the spleens of mice that had rejected the

tumors produced IFN-γ when co-cultured with the mutant epitopes. These peptides were then used as vaccines, which protected against tumor outgrowth when administered prophylactically or after tumor implantation.

Cancer vaccines have long been promising as an additional weapon in the immunotherapy arsenal. However, numerous cancer vaccine trials have failed in the past perhaps due to an over-reliance on surrogate and subjective endpoints from preclinical studies such as histologic evidence of tumor necrosis or lymphocyte infiltration rather than objective cancer regressions (58). Rosenberg and colleagues estimated an objective response rate of only 2.6% in clinical trials using cancer vaccines in 440 patients (422 had metastatic melanoma) at the National Cancer Institute. However, the peptide vaccines given consisted mostly of melanoma-differentiation antigens (e.g. MART-1, gp100, tyrosinase TRP-2) or cancer-testes antigens (e.g. NY-ESO-1, MAGE-12, Her2/neu, telomerase proteins), not neoantigens. Although some of these previous trials generated high frequencies of antigen reactive T cells, low avidity for these self-antigens due to central tolerance may have limited the anti-tumor activity. Having demonstrated YUMMER1.7's immunogenicity and the immune-mediated durable regression of established tumors, we believe YUMMER1.7 to be an appropriate model to investigate the value of neoantigen-based vaccines.

Collectively, our findings point toward a highly immunogenic composition of immune infiltration within YUMMER1.7 tumors. The presence of a functional, activated T cell population in tumors make YUMMER1.7 a valuable tool for studying modifiers of the immune system such as immune checkpoint inhibitors and other therapeutics. Immune checkpoint blockade with ipilimumab, nivolumab and pembrolizumab has led to tumor regression and prolonged overall survival in patients with advanced melanoma and other

malignancies (28, 59). To validate YUMMER1.7 as a model for evaluating immune therapies, we treated 500,000 cell YUMMER1.7 tumors with anti-CTLA-4 and anti-PD-1 therapy. When administered individually or as a combination, these treatments not only inhibited tumor growth but also induced regression and cure of melanoma in a proportion of mice. The combination of anti-CTLA-4 and anti-PD-1 did not significantly delay tumor growth in the less immunogenic YUMM1.7 model. CTLA-4 is believed to regulate immune responses by outcompeting CD28 for their ligands, CD80 and CD86, preventing adequate costimulation of naïve T cells (23). Because CD4 and CD8 T cells are able to infiltrate YUMMER1.7 tumors to a greater extent than in YUMM1.7 tumors, blockade of CTLA-4 may have a stronger effect in the former model. In fact, the density of tumor infiltrating CD8 T cells is one of the best predictors of response to anti-CTLA-4 (60). If the neoantigens in YUMM1.7 do not bind MHC complexes with high affinity, enhanced costimulation may be insufficient to produce an antitumor response. CTLA-4 blockade may also impair immunosuppressive effects of Foxp3+ regulatory T cells in YUMMER1.7 tumors. CTLA-4 has been shown to be constitutively expressed on regulatory T cells and critical for their function (61, 62). Moreover, we observed increased PD1+ TIGIT+ CD8 T cells in YUMMER1.7, reflecting either an activated or exhausted state of cytotoxic T cells. PD-1 blockade may exert its effect by reversing the exhausted subset by inhibiting downstream signaling of the PD-1 receptor and recruitment of the phosphatase SHP-2. YUMMER1.7 demonstrates how immune therapies may shift the balance between immune surveillance and cancer cell growth.

Although responses to checkpoint blockade are often durable and last for years, acquired resistance to these treatments has been documented (63, 64). Several studies suggest

that loss of beta-2-microglobulin, a component of MHC class I molecules, or downregulation of antigens through epigenetic regulation or selection of tumor subclones are potential mechanisms of acquired resistance (65-68). In a recent report, four paired tumor samples (before therapy and after disease progression) that exhibited late acquired resistance after more than 6 months of partial tumor response despite continuous anti-PD-1 therapy were exome sequenced (69). In one tumor pair, a homozygous frame-shift deletion in exon 1 of beta-2-microglobulin caused loss of plasma membrane localization of MHC class I heavy chains in the relapsed tumor. YUMMER1.7 is an ideal model for addressing cancer immunoediting and acquired resistance to therapy. Employing CRISPR/Cas9, beta-2-microglobulin or immunogenic epitopes can be knocked down in YUMMER1.7 tumors to reduce immunogenicity. And inducible forms of CRISPR/Cas9 technology could allow for modulation of the anti-tumor response during treatment through precise temporal control of gene expression (70).

Last of all, the YUMMER1.7 cell line can be used for the evaluation of promising immunotherapies still in development. For example, other T cell inhibitory receptors including LAG-3, TIM-3, VISTA and stimulatory receptors ICOS, OX40, 4-1BB are potential targets. Additional therapies focusing on innate immune activation such as CD40 and STING (stimulator of interferon genes) agonists have drawn great interest. CD40 plays a role in the maturation of antigen presenting cells as well as B cell activation, whereas STING is a cytosolic DNA/damage-associated molecular pattern (DAMP) sensing pathway that drives type I interferon production and activation of Batf3 dendritic cells, which can cross-present to cytotoxic CD8 T cells (71, 72). Similarly, since CSF-1R inhibition is believed to deplete immunosuppressive tumor-associated macrophages in tumors, we presented

preliminary data here that supports the beneficial effect of combining PD-L1 and CSF-1R inhibitors in YUMMER1.7. With no shortage of immunotherapies in the pipeline, a mouse melanoma model that is experimentally tractable for preclinical testing is critical.

For all of these reasons, we anticipate that YUMMER1.7 will serve the scientific community well and be a valuable addition to the YUMM series. It illustrates the role that antigen burden plays in dictating the extent of the anti-tumor immune response and offers the opportunity to study the immune microenvironment with the goal of developing novel immunotherapies. Finally, the described approach used to enhance immunogenicity of the YUMM1.7 line could also be applied to other syngeneic mouse models of cancer.

References

1. Bennett JP, and Hall P. Moles and melanoma: a history. *Ann R Coll Surg Engl.* 1994;76(6):373-80.
2. Chin L, Merlino G, and DePinho RA. Malignant melanoma: modern black plague and genetic black box. *Genes & development.* 1998;12(22):3467-81.
3. Cannon-Albright LA, Goldgar DE, Meyer LJ, Lewis CM, Anderson DE, Fountain JW, Hegi ME, Wiseman RW, Petty EM, Bale AE, et al. Assignment of a locus for familial melanoma, MLM, to chromosome 9p13-p22. *Science.* 1992;258(5085):1148-52.
4. Tsao H, Chin L, Garraway LA, and Fisher DE. Melanoma: from mutations to medicine. *Genes & development.* 2012;26(11):1131-55.
5. Mitra D, Luo X, Morgan A, Wang J, Hoang MP, Lo J, Guerrero CR, Lennerz JK, Mihm MC, Wargo JA, et al. An ultraviolet-radiation-independent pathway to melanoma carcinogenesis in the red hair/fair skin background. *Nature.* 2012;491(7424):449-53.
6. Davies H, Bignell GR, Cox C, Stephens P, Edkins S, Clegg S, Teague J, Woffendin H, Garnett MJ, Bottomley W, et al. Mutations of the BRAF gene in human cancer. *Nature.* 2002;417(6892):949-54.
7. Martincorena I, and Campbell PJ. Somatic mutation in cancer and normal cells. *Science.* 2015;349(6255):1483-9.
8. Shain AH, Yeh I, Kovalyshyn I, Sriharan A, Talevich E, Gagnon A, Dummer R, North J, Pincus L, Ruben B, et al. The Genetic Evolution of Melanoma from Precursor Lesions. *The New England journal of medicine.* 2015;373(20):1926-36.

9. Dankort D, Curley DP, Cartlidge RA, Nelson B, Karnezis AN, Damsky WE, Jr., You MJ, DePinho RA, McMahon M, and Bosenberg M. Braf(V600E) cooperates with Pten loss to induce metastatic melanoma. *Nature genetics.* 2009;41(5):544-52.

10. Garraway LA, Widlund HR, Rubin MA, Getz G, Berger AJ, Ramaswamy S, Beroukhim R, Milner DA, Granter SR, Du J, et al. Integrative genomic analyses identify MITF as a lineage survival oncogene amplified in malignant melanoma. *Nature.* 2005;436(7047):117-22.

11. Shain AH, and Bastian BC. From melanocytes to melanomas. *Nat Rev Cancer.* 2016;16(6):345-58.

12. Cancer Genome Atlas N. Genomic Classification of Cutaneous Melanoma. *Cell.* 2015;161(7):1681-96.

13. Krauthammer M, Kong Y, Ha BH, Evans P, Bacchiocchi A, McCusker JP, Cheng E, Davis MJ, Goh G, Choi M, et al. Exome sequencing identifies recurrent somatic RAC1 mutations in melanoma. *Nature genetics.* 2012;44(9):1006-14.

14. Vogelstein B, Papadopoulos N, Velculescu VE, Zhou S, Diaz LA, Jr., and Kinzler KW. Cancer genome landscapes. *Science.* 2013;339(6127):1546-58.

15. Schumacher TN, and Schreiber RD. Neoantigens in cancer immunotherapy. *Science.* 2015;348(6230):69-74.

16. Forbes SA, Beare D, Gunasekaran P, Leung K, Bindal N, Boutselakis H, Ding M, Bamford S, Cole C, Ward S, et al. COSMIC: exploring the world's knowledge of somatic mutations in human cancer. *Nucleic Acids Res.* 2015;43(Database issue):D805-11.

17. Sondak VK, Glass LF, and Geller AC. Risk-stratified screening for detection of melanoma. *JAMA.* 2015;313(6):616-7.

18. Chapman PB, Hauschild A, Robert C, Haanen JB, Ascierto P, Larkin J, Dummer R, Garbe C, Testori A, Maio M, et al. Improved survival with vemurafenib in melanoma with BRAF V600E mutation. *The New England journal of medicine.* 2011;364(26):2507-16.

19. Lo JA, and Fisher DE. The melanoma revolution: from UV carcinogenesis to a new era in therapeutics. *Science.* 2014;346(6212):945-9.

20. Atkins MB, Lotze MT, Dutcher JP, Fisher RI, Weiss G, Margolin K, Abrams J, Sznol M, Parkinson D, Hawkins M, et al. High-dose recombinant interleukin 2 therapy for patients with metastatic melanoma: analysis of 270 patients treated between 1985 and 1993. *J Clin Oncol.* 1999;17(7):2105-16.

21. Walunas TL, Lenschow DJ, Bakker CY, Linsley PS, Freeman GJ, Green JM, Thompson CB, and Bluestone JA. CTLA-4 can function as a negative regulator of T cell activation. *Immunity.* 1994;1(5):405-13.

22. Krummel MF, and Allison JP. CD28 and CTLA-4 have opposing effects on the response of T cells to stimulation. *J Exp Med.* 1995;182(2):459-65.

23. Pardoll DM. The blockade of immune checkpoints in cancer immunotherapy. *Nat Rev Cancer.* 2012;12(4):252-64.

24. Hodi FS, O'Day SJ, McDermott DF, Weber RW, Sosman JA, Haanen JB, Gonzalez R, Robert C, Schadendorf D, Hassel JC, et al. Improved survival with ipilimumab in patients with metastatic melanoma. *The New England journal of medicine.* 2010;363(8):711-23.

25. Chen L, and Han X. Anti-PD-1/PD-L1 therapy of human cancer: past, present, and future. *J Clin Invest.* 2015;125(9):3384-91.

26. Robert C, Long GV, Brady B, Dutriaux C, Maio M, Mortier L, Hassel JC, Rutkowski P, McNeil C, Kalinka-Warzocha E, et al. Nivolumab in previously untreated melanoma without BRAF mutation. *The New England journal of medicine.* 2015;372(4):320-30.

27. Robert C, Schachter J, Long GV, Arance A, Grob JJ, Mortier L, Daud A, Carlino MS, McNeil C, Lotem M, et al. Pembrolizumab versus Ipilimumab in Advanced Melanoma. *The New England journal of medicine.* 2015;372(26):2521-32.

28. Wolchok JD, Kluger H, Callahan MK, Postow MA, Rizvi NA, Lesokhin AM, Segal NH, Ariyan CE, Gordon RA, Reed K, et al. Nivolumab plus ipilimumab in advanced melanoma. *The New England journal of medicine.* 2013;369(2):122-33.

29. Larkin J, Chiarion-Sileni V, Gonzalez R, Grob JJ, Cowey CL, Lao CD, Schadendorf D, Dummer R, Smylie M, Rutkowski P, et al. Combined Nivolumab and Ipilimumab or Monotherapy in Untreated Melanoma. *The New England journal of medicine.* 2015;373(1):23-34.

30. Postow MA, Chesney J, Pavlick AC, Robert C, Grossmann K, McDermott D, Linette GP, Meyer N, Giguere JK, Agarwala SS, et al. Nivolumab and ipilimumab versus ipilimumab in untreated melanoma. *The New England journal of medicine.* 2015;372(21):2006-17.

31. Lawrence MS, Stojanov P, Polak P, Kryukov GV, Cibulskis K, Sivachenko A, Carter SL, Stewart C, Mermel CH, Roberts SA, et al. Mutational heterogeneity in cancer and the search for new cancer-associated genes. *Nature.* 2013;499(7457):214-8.

32. Le DT, Uram JN, Wang H, Bartlett BR, Kemberling H, Eyring AD, Skora AD, Luber BS, Azad NS, Laheru D, et al. PD-1 Blockade in Tumors with Mismatch-Repair Deficiency. *The New England journal of medicine.* 2015;372(26):2509-20.

33. Van Allen EM, Miao D, Schilling B, Shukla SA, Blank C, Zimmer L, Sucker A, Hillen U, Geukes Foppen MH, Goldinger SM, et al. Genomic correlates of response to CTLA-4 blockade in metastatic melanoma. *Science.* 2015;350(6257):207-11.

34. Snyder A, Makarov V, Merghoub T, Yuan J, Zaretsky JM, Desrichard A, Walsh LA, Postow MA, Wong P, Ho TS, et al. Genetic basis for clinical response to CTLA-4 blockade in melanoma. *The New England journal of medicine.* 2014;371(23):2189-99.

35. McGranahan N, Furness AJ, Rosenthal R, Ramskov S, Lyngaa R, Saini SK, Jamal-Hanjani M, Wilson GA, Birkbak NJ, Hiley CT, et al. Clonal neoantigens elicit T cell immunoreactivity and sensitivity to immune checkpoint blockade. *Science.* 2016;351(6280):1463-9.

36. Damsky WE, Jr., and Bosenberg M. Mouse melanoma models and cell lines. *Pigment cell & melanoma research.* 2010;23(6):853-9.

37. Harding HE, Passey, R. D. A transplantable melanoma of the mouse. *J Pathol Bacteriol.* 1930;33(417-27.

38. Castle JC, Kreiter S, Diekmann J, Lower M, van de Roemer N, de Graaf J, Selmi A, Diken M, Boegel S, Paret C, et al. Exploiting the mutanome for tumor vaccination. *Cancer research.* 2012;72(5):1081-91.

39. Kershaw MH, Hsu C, Mondesire W, Parker LL, Wang G, Overwijk WW, Lapointe R, Yang JC, Wang RF, Restifo NP, et al. Immunization against endogenous retroviral tumor-associated antigens. *Cancer research.* 2001;61(21):7920-4.

40. Li M, Huang X, Zhu Z, and Gorelik E. Sequence and insertion sites of murine melanoma-associated retrovirus. *J Virol.* 1999;73(11):9178-86.

41. Becker JC, Houben R, Schrama D, Voigt H, Ugurel S, and Reisfeld RA. Mouse models for melanoma: a personal perspective. *Exp Dermatol.* 2010;19(2):157-64.

42. van Elsas A, Hurwitz AA, and Allison JP. Combination immunotherapy of B16 melanoma using anti-cytotoxic T lymphocyte-associated antigen 4 (CTLA-4) and granulocyte/macrophage colony-stimulating factor (GM-CSF)-producing vaccines induces rejection of subcutaneous and metastatic tumors accompanied by autoimmune depigmentation. *J Exp Med.* 1999;190(3):355-66.

43. Nogueira C, Kim KH, Sung H, Paraiso KH, Dannenberg JH, Bosenberg M, Chin L, and Kim M. Cooperative interactions of PTEN deficiency and RAS activation in melanoma metastasis. *Oncogene.* 2010;29(47):6222-32.

44. VanBrocklin MW, Robinson JP, Lastwika KJ, Khoury JD, and Holmen SL. Targeted delivery of NRASQ61R and Cre-recombinase to post-natal melanocytes induces melanoma in Ink4a/Arflox/lox mice. *Pigment cell & melanoma research.* 2010;23(4):531-41.

45. Meeth K, Wang JX, Micevic G, Damsky W, and Bosenberg MW. The YUMM lines: a series of congenic mouse melanoma cell lines with defined genetic alterations. *Pigment cell & melanoma research.* 2016;29(5):590-7.

46. Ho PC, Bihuniak JD, Macintyre AN, Staron M, Liu X, Amezquita R, Tsui YC, Cui G, Micevic G, Perales JC, et al. Phosphoenolpyruvate Is a Metabolic Checkpoint of Anti-tumor T Cell Responses. *Cell.* 2015;162(6):1217-28.

47. Homet Moreno B, Zaretsky JM, Garcia-Diaz A, Tsoi J, Parisi G, Robert L, Meeth K, Ndoye A, Bosenberg M, Weeraratna AT, et al. Response to Programmed Cell Death-1 Blockade in a Murine Melanoma Syngeneic Model Requires Costimulation, CD4, and CD8 T Cells. *Cancer immunology research.* 2016;4(10):845-57.

48. Scortegagna M, Lau E, Zhang T, Feng Y, Sereduk C, Yin H, De SK, Meeth K, Platt JT, Langdon CG, et al. PDK1 and SGK3 Contribute to the Growth of BRAF-Mutant Melanomas and Are Potential Therapeutic Targets. *Cancer research.* 2015;75(7):1399-412.

49. Satoh S, Hashimoto-Tamaoki T, Furuyama J, Mihara K, Namba M, and Kitano Y. High frequency of tetraploidy detected in malignant melanoma of Japanese patients by fluorescence in situ hybridization. *Int J Oncol.* 2000;17(4):707-15.

50. Day CP, Merlino G, and Van Dyke T. Preclinical mouse cancer models: a maze of opportunities and challenges. *Cell.* 2015;163(1):39-53.

51. Mestas J, and Hughes CC. Of mice and not men: differences between mouse and human immunology. *J Immunol.* 2004;172(5):2731-8.

52. Ward JP, Gubin MM, and Schreiber RD. The Role of Neoantigens in Naturally Occurring and Therapeutically Induced Immune Responses to Cancer. *Adv Immunol.* 2016;130(25-74.

53. Utzschneider DT, Alfei F, Roelli P, Barras D, Chennupati V, Darbre S, Delorenzi M, Pinschewer DD, and Zehn D. High antigen levels induce an exhausted phenotype in a

chronic infection without impairing T cell expansion and survival. *J Exp Med.* 2016;213(9):1819-34.

54. Holmgaard RB, Zamarin D, Li Y, Gasmi B, Munn DH, Allison JP, Merghoub T, and Wolchok JD. Tumor-Expressed IDO Recruits and Activates MDSCs in a Treg-Dependent Manner. *Cell reports.* 2015;13(2):412-24.

55. Lahl K, and Sparwasser T. In vivo depletion of FoxP3+ Tregs using the DEREG mouse model. *Methods in molecular biology.* 2011;707(157-72.

56. Buus S, Lauemoller SL, Worning P, Kesmir C, Frimurer T, Corbet S, Fomsgaard A, Hilden J, Holm A, and Brunak S. Sensitive quantitative predictions of peptide-MHC binding by a 'Query by Committee' artificial neural network approach. *Tissue Antigens.* 2003;62(5):378-84.

57. Gubin MM, Zhang X, Schuster H, Caron E, Ward JP, Noguchi T, Ivanova Y, Hundal J, Arthur CD, Krebber WJ, et al. Checkpoint blockade cancer immunotherapy targets tumour-specific mutant antigens. *Nature.* 2014;515(7528):577-81.

58. Rosenberg SA, Yang JC, and Restifo NP. Cancer immunotherapy: moving beyond current vaccines. *Nat Med.* 2004;10(9):909-15.

59. Sharma P, and Allison JP. The future of immune checkpoint therapy. *Science.* 2015;348(6230):56-61.

60. Ji RR, Chasalow SD, Wang L, Hamid O, Schmidt H, Cogswell J, Alaparthy S, Berman D, Jure-Kunkel M, Siemers NO, et al. An immune-active tumor microenvironment favors clinical response to ipilimumab. *Cancer Immunol Immunother.* 2012;61(7):1019-31.

61. Takahashi T, Tagami T, Yamazaki S, Uede T, Shimizu J, Sakaguchi N, Mak TW, and Sakaguchi S. Immunologic self-tolerance maintained by CD25(+)CD4(+) regulatory T cells constitutively expressing cytotoxic T lymphocyte-associated antigen 4. *J Exp Med.* 2000;192(2):303-10.

62. Wing K, Onishi Y, Prieto-Martin P, Yamaguchi T, Miyara M, Fehervari Z, Nomura T, and Sakaguchi S. CTLA-4 control over Foxp3+ regulatory T cell function. *Science.* 2008;322(5899):271-5.

63. Prieto PA, Yang JC, Sherry RM, Hughes MS, Kammula US, White DE, Levy CL, Rosenberg SA, and Phan GQ. CTLA-4 blockade with ipilimumab: long-term follow-up of 177 patients with metastatic melanoma. *Clinical cancer research : an official journal of the American Association for Cancer Research.* 2012;18(7):2039-47.

64. Ribas A. Adaptive Immune Resistance: How Cancer Protects from Immune Attack. *Cancer discovery.* 2015;5(9):915-9.

65. Schreiber RD, Old LJ, and Smyth MJ. Cancer immunoediting: integrating immunity's roles in cancer suppression and promotion. *Science.* 2011;331(6024):1565-70.

66. Matsushita H, Vesely MD, Koboldt DC, Rickert CG, Uppaluri R, Magrini VJ, Arthur CD, White JM, Chen YS, Shea LK, et al. Cancer exome analysis reveals a T-cell-dependent mechanism of cancer immunoediting. *Nature.* 2012;482(7385):400-4.

67. DuPage M, Mazumdar C, Schmidt LM, Cheung AF, and Jacks T. Expression of tumour-specific antigens underlies cancer immunoediting. *Nature.* 2012;482(7385):405-9.

68. Rooney MS, Shukla SA, Wu CJ, Getz G, and Hacohen N. Molecular and genetic properties of tumors associated with local immune cytolytic activity. *Cell.* 2015;160(1-2):48-61.

69. Zaretsky JM, Garcia-Diaz A, Shin DS, Escuin-Ordinas H, Hugo W, Hu-Lieskovan S, Torrejon DY, Abril-Rodriguez G, Sandoval S, Barthly L, et al. Mutations Associated with Acquired Resistance to PD-1 Blockade in Melanoma. *The New England journal of medicine.* 2016;375(9):819-29.

70. Cao J, Wu L, Zhang SM, Lu M, Cheung WK, Cai W, Gale M, Xu Q, and Yan Q. An easy and efficient inducible CRISPR/Cas9 platform with improved specificity for multiple gene targeting. *Nucleic Acids Res.* 2016;44(19):e149.

71. Mahoney KM, Rennert PD, and Freeman GJ. Combination cancer immunotherapy and new immunomodulatory targets. *Nat Rev Drug Discov.* 2015;14(8):561-84.

72. Corrales L, Matson V, Flood B, Spranger S, and Gajewski TF. Innate immune signaling and regulation in cancer immunotherapy. *Cell Res.* 2017;27(1):96-108.